TU Delft

Delft University of Technology

Document Version
Final published version

Licence
CC BY

Citation (APA)
Papanikolaou, N., Saccone, C., & Pahlavan, L. (2026). Impact Identification in Thin-Walled Structures Using Time Reversal of Guided Waves. In *Proceedings of the 12th European Workshop on Structural Health Monitoring (EWSHM 2026): July 7-10, 2026 in Toulouse, France* Article 1196 (e-Journal of Nondestructive Testing; Vol. 2026, No. 08). NDT.net. https://doi.org/10.58286/33705

Important note
To cite this publication, please use the final published version (if applicable).
Please check the document version above.

Copyright
In case the licence states “Dutch Copyright Act (Article 25fa)”, this publication was made available Green Open Access via the TU Delft Institutional Repository pursuant to Dutch Copyright Act (Article 25fa, the Taverne amendment). This provision does not affect copyright ownership.
Unless copyright is transferred by contract or statute, it remains with the copyright holder.

Sharing and reuse
Other than for strictly personal use, it is not permitted to download, forward or distribute the text or part of it, without the consent of the author(s) and/or copyright holder(s), unless the work is under an open content license such as Creative Commons.

Takedown policy
Please contact us and provide details if you believe this document breaches copyrights.
We will remove access to the work immediately and investigate your claim.

This work is downloaded from Delft University of Technology.

More info about this article: https://www.ndt.net/?id=33705

Impact Identification in Thin-Walled Structures Using Time Reversal of Guided Waves

Nikolaos PAPANIKOLAOU[1], Cecilia SACCONE[1], Lotfollah PAHLAVAN[1]
[1] Delft University of Technology, Delft, Netherlands,
N.Papanikolaou@tudelft.nl, C.Saccone@tudelft.nl, L.Pahlavan@tudelft.nl

Abstract. This paper presents a framework for impact source localization and force reconstruction in stiffened thin-walled steel structures using Guided Waves. Impact localization is performed using passive Time Reversal in the frequency domain, enabling the source signal reconstruction for subsequent force estimation. Force reconstruction is achieved using a parametric half-sine model combined with a transfer function obtained from a single calibration impact.
The approach is experimentally validated on a steel plate subjected to controlled impacts while monitoring its structural response using piezoelectric sensors. The results show that impact localization can be achieved with mean errors of 14.7 mm and 23.7 mm for the plate and stiffened configurations, respectively. More than 80% of the impacts are localized within 10% of the sensor spacing. The reconstructed forces using the parametric model provide an estimate of the applied impact force, with a mean relative error of approximately 31%.
The results demonstrate that the proposed approach can enable combined impact localization and force estimation in thin-walled structures, with and without the presence of structural stiffeners.

Keywords: Time Reversal, impact localization, force reconstruction

Introduction

Marine structures operate in a complex environment facing the risk of impacts. Localizing impacts and quantifying their energy is essential for the effective reliability and integrity assessment of these structures. During impact, energy is dissipated through several mechanisms including deformation, sound emission, structural vibration and elastic stress waves. In thin-walled structures such as ships, the latter partly propagate as Guided Waves (GWs) which can travel long distances with limited attenuation.

Due to this propagation characteristic, GWs have been extensively employed for the Structural Health Monitoring (SHM) of large-scale structures such as bridges [1,2], offshore platforms [3,4] and pipelines [5]. Their ability to transfer meaningful information across long distances has motivated their use for impact identification in this research, including both impact source localization and impact force reconstruction.

For source localization, geometrical methods, often referred to in the literature as triangulation, have been widely used [6]. However, their accuracy deteriorates when co-existing wave modes, dispersion, thickness variations, geometric irregularities and noise are encountered [7,8]. Time Reversal (TR) has emerged as a robust alternative exploiting the time reversibility and spatial reciprocity properties of wave propagation, which allow GWs generated by point-like impacts to refocus on the impact source [9,10]. In thin-walled structures, source localization with TR has been realized either using Impulse Response Functions [8,11–13], or through the numerical back-propagation of the transient responses to reconstruct the wavefield and localize the source [7,14,15].

This work is licensed under CC BY 4.0

Media and Publishing Partner NDT.net
https://doi.org/10.58286/33705

Following source localization, the next step is to reconstruct the impact force. This involves solving an inverse problem, in which the force time history and magnitude are estimated from the measured structural responses. Among the available approaches found in the literature [16,17], direct methods retrieve the input force by formulating the inverse problem using physical or mathematical models of the structure [18–20], while deconvolution methods retrieve the input force through the deconvolution of the measured response with the transfer function of the structure [21], which can be obtained experimentally [22] or numerically [23].

This paper presents a combined framework for impact source localization and force reconstruction on steel plates and stiffened panels representative of ship hull structures. TR impact localization is performed in the frequency domain followed by parametric force reconstruction using the TR-reconstructed source at the identified impact location. The approach is validated experimentally on small-scale controlled impact experiments. The paper is organised as follows. The approach is described in Section 1. The experimental setup is described in Section 2. Results are presented and discussed in Section 3, followed by conclusions in Section 4.

1. Methodology

Impacts on thin-walled structures generate stress waves that propagate over long distances as dispersive multimodal GWs. In plate-like structures, GWs exist as symmetric (S), antisymmetric (A) and shear horizontal modes (SH).

In the frequency domain the measured signal P at a sensor can be expressed as the convolution of the sensor transfer function D with the medium transfer function W and the impact-induced source signal S, plus a noise component N [24,25]. For M propagating modes, the measured signal is given through their superposition, as given in Equation (1).

$$\mathrm{P}(\omega) = \sum_{m=1}^{M} D_m(\omega) W_m(d_k, \omega) S(\omega) + N(\omega) \tag{1}$$

where $\omega = 2\pi f$ is the angular frequency with f being the frequency, $m = 1, \ldots, M$ are the propagating modes and d_k is the propagation distance.

The medium transfer function of a single propagating wave mode over a distance d_k is given in Equation (2), and accounts both for dispersion and amplitude decay due to geometric spreading.

$$W(d_k, \omega) = exp\left(-i\omega d_k / c_p(\omega)\right) \sqrt{L_{\mathrm{ref}}/d_k} \tag{2}$$

where $c_p(\omega)$ is the frequency dependent phase velocity, and L_{ref} is the reference near-field dimension.

Although multiple wave modes may co-exist, it is often possible to design or select piezoelectric sensors to be primarily sensitive to a specific wave mode [10]. Without loss of generality, in this study the propagation is approximated using a single dominant wave mode, simplifying the wavefield reconstruction process.

When GWs interact with structural features such as stiffeners, phenomena such as transmission losses, wave scattering and mode conversion are encountered [26]. In this study, these are accounted for using a transmission coefficient $T(\alpha, \omega)$ dependent on the angle of incidence α of the waves on the stiffener and the angular frequency ω [27]. For a propagation path crossing n stiffeners, as shown in Figure 1 the measured signal P_k at sensor k can be expressed through Equation (3) [27].

$$P_k(\omega) = D_k(\omega) T^n(\alpha, \omega) W(d_k, \omega) S(\omega) + N(\omega) \tag{3}$$

Measurement noise and unmodeled terms such as reflections, scatterings and mode conversions are partially mitigated through signal processing (band-pass filtering and windowing) and are neglected in the following derivations.

This work is licensed under CC BY 4.0

Media and Publishing Partner NDT.net

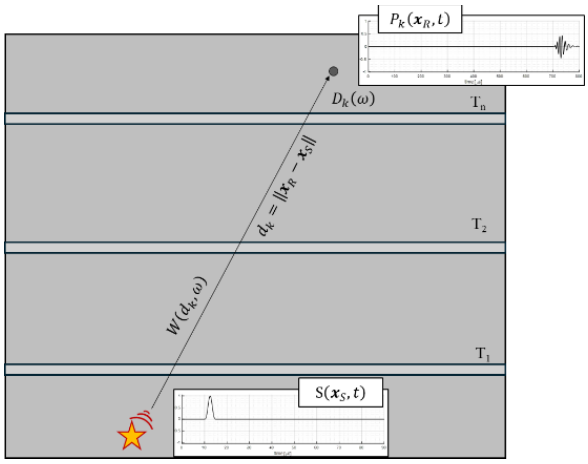


Figure 1: Schematic of impact induced GW transmission through stiffeners in a stiffened steel panel.

1.1 Wavefield Reconstruction and Impact Localization

Impact identification is performed exploiting the TR property of GWs. The method exploits two fundamental properties of elastic wave propagation, time reversibility and spatial reciprocity, which allow GWs generated by point-like impacts to refocus on their origin [10].

In the frequency domain, time reversal of a function is equivalent to its complex conjugation. The recorded transient responses are therefore conjugated and back-propagated from the sensor locations to candidate locations into the monitored domain. The back-propagation is performed using the transfer function W while compensating for sensor response, geometric spreading, and transmission losses. The reconstructed signal at an arbitrary location is estimated by averaging the contributions from the N_s sensors, given by Equation (4).

$$S_{rec}(\omega) = \frac{1}{N_s}\sum_{k=1}^{N_s} T^{-n}(\alpha,\omega)\frac{1}{D_k^*(\omega)}\frac{d_k}{L_{\text{ref}}}W(\omega)P_k^*(\omega) \tag{4}$$

where $(\quad)^*$ denotes complex conjugation, d_k/L_{ref} compensation for geometric spreading, $1/D_k^*(\omega)$ sensor transfer function compensation, and $T^{-n}(\alpha,\omega)$ compensation for transmission losses at n stiffeners.

According to the TR property, the reconstructed wavefield theoretically attains its maximum amplitude at the original impact location. The monitoring area enclosed by the sensors Ω is discretized into a uniform spatial grid and Equation (4) is evaluated at each grid point. The impact location $\boldsymbol{x}_{source}$ is identified as the grid point where the reconstructed source attains its peak amplitude over both space and time as described in Equation (5).

$$\boldsymbol{x}_{source} = arg\max_{\boldsymbol{x}\in\Omega,\mathbf{t}}|S_{rec}(t)| \tag{5}$$

1.2 Impact Force Reconstruction

Following source localization, the impact force is estimated using the reconstructed signal at the identified impact location. The TR process in principle is a deconvolution technique since the dispersion effects are inherently compensated for during the back-propagation. This allows the reconstructed signal to be directly related to the input force using a transfer function $H(\omega)$, obtained through calibration impacts.

In practice however, this is not always feasible as the frequency content of the impact force is mostly dominated by low-frequency components (<10 kHz), while the piezoelectric sensors are sensitive to higher frequency components. As a result, the measured spectra may not overlap, making their direct relation ill-conditioned.

To address this limitation, the impact force is modelled analytically using a half-sine pulse parametrized with F_0 and contact duration T_c [28]. This representation allows its spectrum to be

evaluated in the frequency range where the sensors are most sensitive. Equation (6) and Equation (7) show the half-sine pulse in the time and frequency domain respectively.

$$F(t) = F_0 \sin\left(\frac{\pi}{T_c} t\right), 0 \le t \le T_c \tag{6}$$

$$\hat{F}(\omega, F_0, T_c) = \frac{\mathrm{F_0}\omega_\mathrm{f}}{\omega_\mathrm{f}^2 - \omega^2}[1 + exp(-i\omega T_c)] \tag{7}$$

where, $\omega_\mathrm{f} = \pi/T_c$ is the half sine pulse forcing frequency.

A calibration impact is performed at a known location using the instrumented hammer, providing the applied force time history while measuring the piezoelectric sensor response. Using the proposed TR approach, the impact is localized and the source signal S_{rec} is reconstructed. Therefore, the transfer function $H(\omega)$ can be estimated with Equation (8) in the piezoelectric sensors' supported frequency band using the Fourier transform of the analytical model, even though the physical force contribution in that frequency range may be insignificant. $\hat{F}(\omega)$ is evaluated using the contact duration T_c and peak force F_0 measured during impact.

$$H(\omega) = \frac{\hat{F}(\omega)}{S_{rec}(\omega)} \tag{8}$$

Assuming accurate compensation of the propagation effects and linear sensor response, $H(\omega)$ can be regarded virtually independent of the impact location and magnitude, allowing a single calibration to be used on all impacts. For each impact, the force spectrum is as follows:

$$\mathrm{F_{est}}(\omega) = H(\omega) S_{rec}(\omega) \tag{9}$$

Finally, the parameters F_0 and T_c are estimated by fitting the half-sine model to the estimated force spectrum $F_{est}(\omega)$ using nonlinear least squares minimization. Finally, the impact force time history is obtained directly by substituting the fitted parameters into Equation (6). The complete localization and force reconstruction framework is summarized in Figure 2.

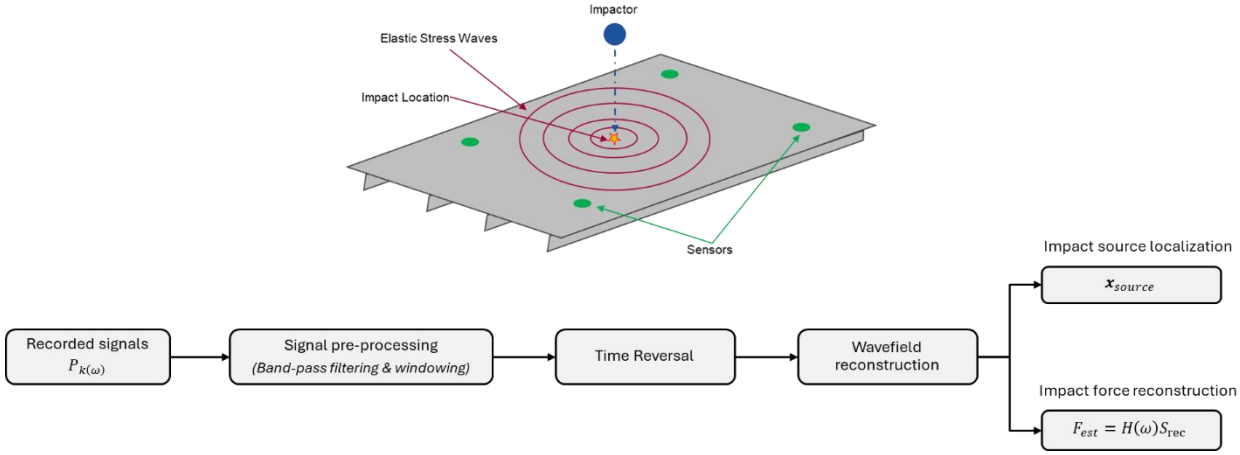


Figure 2: Overview of the proposed methodology.

2. Experiments

Experimental validation was performed using the setup shown in Figure 3. The structure is a high strength steel (S355) plate representative of the inner part of a ship hull. The base plate measures 1700x1200x10mm^3. A 7 mm thick bulb profile stiffener is welded on the plate and intersects with a 100x8mm^2 cross section flange.

Four surface-mounted 60 kHz (R6α) piezoelectric sensors were attached to the structure using magnetic holders to record the waves generated during impact. The sensors were arranged in a rectangular array enclosing an area of 400×400 mm^2. Elastic waves were generated using an

instrumented hammer equipped with a steel tip allowing the simultaneous measurement of the input force and the structural response.

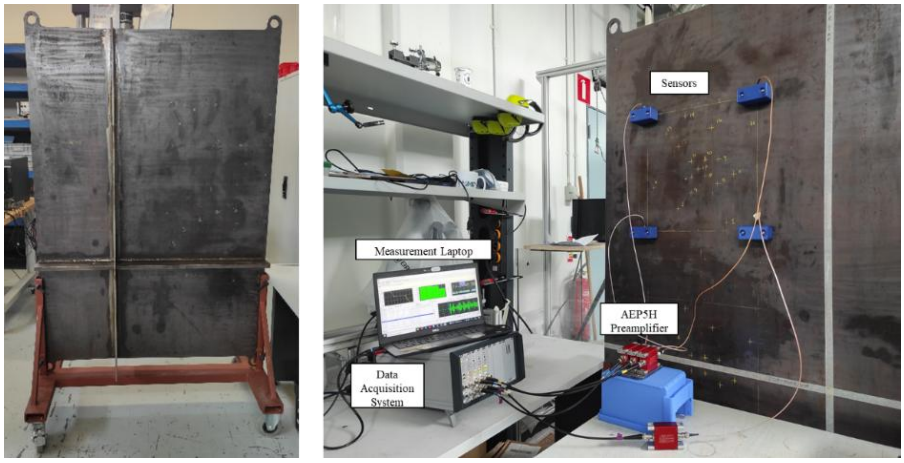


Figure 3: Experimental setup and instrumentation.

To assess the method under increasing structural complexity, the two configurations shown in Figure 4 were investigated. In the first configuration, the sensors were arranged in such way that the paths between the impact location and the sensors did not interfere with the stiffeners. In the second configuration the propagation path between the impact location and the sensors crossed the stiffener introducing transmission effects.

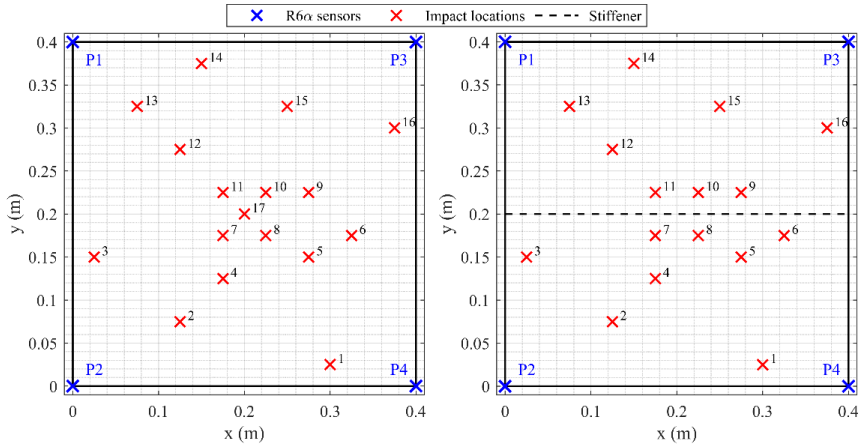


Figure 4: Controlled impact locations. Plate configuration (left); Stiffened plate configuration (right).

3. Results and Discussion

Impact identification was performed according to the proposed methodology in Section 1. In the frequency range of interest (<100 kHz) and plate thickness (10 mm), only the fundamental symmetric (S0) and antisymmetric (A0) wave modes propagate. Single mode localization was performed using the fundamental antisymmetric wave mode (A0), which dominated the recorded signals. This is consistent with the fact that out-of-plane excitation predominantly generates flexural elastic waves. Additionally, surface mounted transducers are more sensitive to the out-of-plane displacement of the plate, further enhancing the A0 wave dominance.

Three impacts were performed per location resulting in a total of 51 and 48 analysed impacts for the plate and stiffened plate configurations, respectively. The monitored area was discretized into a 4×4 mm^2 uniform grid and the wavefield was reconstructed at every location. To isolate the direct wave arrivals, the first 100 μs of the recorded signals were windowed and band-pass filtered between 40-75 kHz to remove the low- and high-frequency noise components, associated with structural vibrations and high frequency measurement noise respectively.

This work is licensed under CC BY 4.0

Media and Publishing Partner

Figure 5 shows the normalized reconstructed wavefields at the time of the impact for a representative impact at location 14 for both configurations. The green cross marks the predicted impact location whereas the actual impact location is indicated with the black plus symbol.

For the plate configuration, the impact locations were predicted with 14.7 ± 18.2 mm error (mean ± standard deviation). In the stiffened plate configuration, the error increased to 23.7 ± 19.8 mm. The presence of the stiffener introduces propagation complexity, affecting the measured signal and reducing the localization accuracy. Nevertheless, the proposed methodology maintains reasonably high localization performance with more than 80% of the test cases localized with less than 40 mm error, corresponding to 10% of the sensor distance.

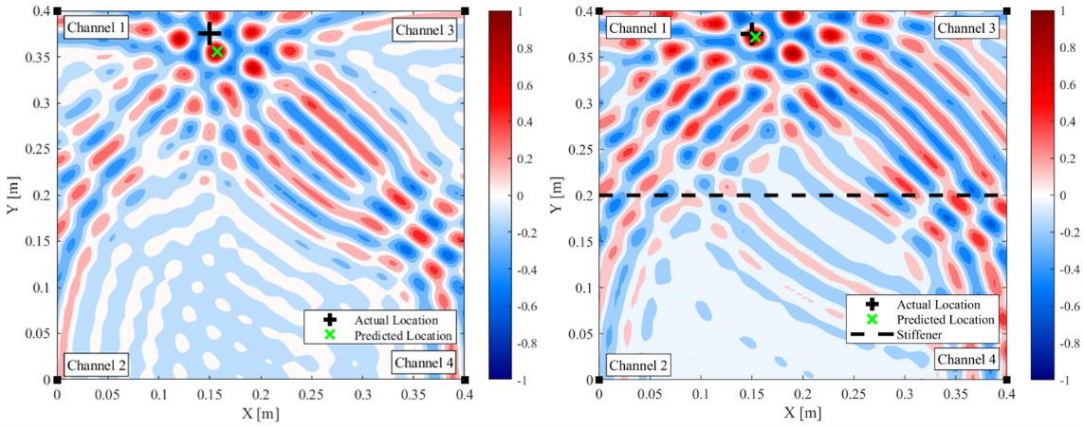


Figure 5: Reconstructed wavefield and predicted impact location. Plate (left) and stiffened plate configuration (right).

Following localization, the impact force was retrieved using the reconstructed source signal at the predicted impact location. Figure 6 shows the measured force signal used for the calibration (Location 17) and its approximation using the half-sine model in both the time and frequency domains. Although the half-sine model does not perfectly capture all the features of the measured signal it is a satisfactory representation of the input force up to frequencies of 15-20 kHz, where most of the impact energy is concentrated.

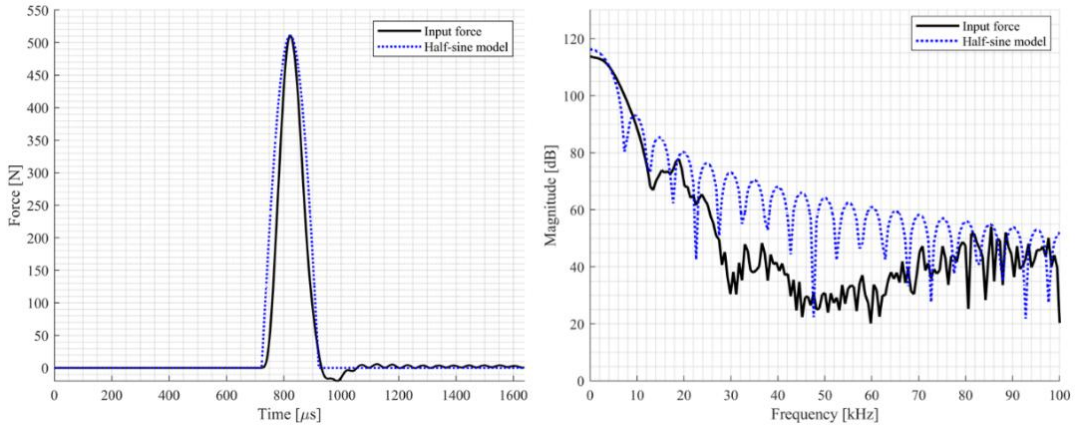


Figure 6: Input force time history (left) and frequency spectrum (right).

Using the calibrated transfer function, the applied force was reconstructed for the test cases in both configurations. Figure 7 compares the reconstructed forces with the measured hammer force signals for representative impacts. The reconstructed force signals follow the temporal shape of the measured forces and in general provide a reasonable estimate of their magnitude. For the stiffened plate configuration, the transmission coefficient T used to compensate for the stiffener transmission effects was assumed to be constant ($T = 0.65$) [27], over the considered range of the angle of incidence and frequency. Despite this simplification, the reconstruction performance remains comparable in both configurations.

This work is licensed under CC BY 4.0

Media and Publishing Partner

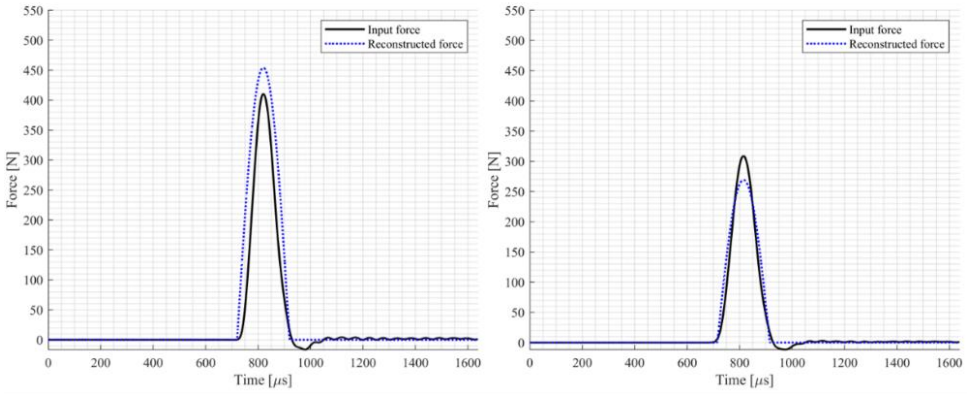


Figure 7: Reconstructed force signals. Location 8 plate (left); Location 10 stiffened plate (right).

Force reconstruction accuracy was quantified using the relative error between the reconstructed and measured peak force. For each impact, the relative error was computed using Equation (10). The mean relative reconstruction error, averaged over all impacts in each configuration with the standard deviation indicating the spread across impacts, was approximately 31.5 ± 25.1% for the plate configuration and 30.6 ± 28.7% for the stiffened plate configuration. Although the calibration impact was performed with a force of approximately 500 N, the proposed approach is able to retrieve forces of various amplitudes ranging between 200 N and 600 N, further supporting that impact force estimation is feasible with a single calibration impact.

$$e_i = \frac{\left|F_{0,rec,i} - F_{0,meas,i}\right|}{F_{0,meas,i}} \times 100\% \tag{10}$$

where $F_{0,rec,i}$ and $F_{0,meas,i}$ are the reconstructed and measured peak forces.

4. Conclusions

This study investigated the feasibility of impact identification in thin-walled structures, representative of ship hulls, using the TR property of GWs. Small-scale experiments were performed on a 10 mm thick plate with and without a longitudinal stiffener. A network consisting of 4 R6α sensors was used to monitor the structure and record the transient structural response from controlled impacts.

Impact source localization was achieved by virtually back-propagating the recorded signals in the frequency domain, using the analytical description of the medium transfer function. The results suggest that accurate localization is possible in both configurations. Although the presence of the stiffener introduces complexities in the wave propagation and increases the localization error, more than 80% of the test cases were localized with errors below 40 mm, corresponding to 10% of the sensor distance.

The input force was retrieved using the reconstructed signal at the impact location and a transfer function obtained from a single calibration impact. The method produces comparable force estimation results in both configurations with a mean relative error of approximately 31% across a range of impact magnitudes, providing an estimate of the impact severity.

Overall, the results demonstrate that the proposed TR-based framework enables impact identification across structures with increasing structural complexity. These findings suggest that passive GW monitoring has application potential in future impact SHM frameworks. Future work will be performed to extend the approach to larger and more complex structures made of isotropic and anisotropic materials.

This work is licensed under CC BY 4.0

Media and Publishing Partner NDT.net

5. Acknowledgements

This research was conducted within the framework of Impact-ID project. Impact-ID has been made possible by the financial contribution of COMMIT. The project partners are acknowledged for their support and contribution.

References

[1] Pahlavan L, Paulissen J, Pijpers R, Hakkesteegt H, Jansen R. Acoustic Emission Health Monitoring of Steel Bridges. In: Le Cam, Vincent, Mevel, Laurent, Schoefs, Franck, editors. EWSHM - 7th European Workshop on Structural Health Monitoring, Nantes, France: 2014.

[2] Nair A, Cai CS. Acoustic emission monitoring of bridges: Review and case studies. Eng Struct 2010;32:1704–14. https://doi.org/10.1016/j.engstruct.2010.02.020.

[3] Grosse CU. Acoustic emission localization methods for large structures based on beamforming and array techniques. Proceedings of the NDTCE 2009.

[4] Mitchell JS, Rogers M. OTC 6957 Monitoring Structural Integrity of North Sea Production Platforms by Acoustic Emission. 1992.

[5] Fromme P. Guided Wave Testing. In: Ida N, Meyendorf N, editors. Handbook of Advanced Nondestructive Evaluation, Springer International Publishing; 2019, p. 141–70. https://doi.org/10.1007/978-3-319-26553-7_24.

[6] Tobias A. Acoustic-emission source location in two dimensions by an array of three sensors. Non-Destructive Testing 1976;9:9–12. https://doi.org/10.1016/0029-1021(76)90027-X.

[7] Yu Z, Sun J, Xu C, Du F. Locating of acoustic emission source for stiffened plates based on stepwise time-reversal processing with time-domain spectral finite element simulation. Struct Health Monit 2023;22:927–47. https://doi.org/10.1177/14759217221094462.

[8] Miniaci M, Mazzotti M, Radzieński M, Kudela P, Kherraz N, Bosia F, et al. Application of a laser-based time reversal algorithm for impact localization in a stiffened aluminum plate. Front Mater 2019;6. https://doi.org/10.3389/fmats.2019.00030.

[9] Fink M. Time Reversal of Ultrasonic Fields-Part I: Basic Principles. IEEE Trans Ultrason Ferroelectr Freq Control 1992;39:555–66.

[10] Xu B, Giurgiutiu V. Single mode tuning effects on lamb wave time reversal with piezoelectric wafer active sensors for structural health monitoring. J Nondestr Eval 2007;26:123–34. https://doi.org/10.1007/s10921-007-0027-8.

[11] Ciampa F, Meo M. Impact detection in anisotropic materials using a time reversal approach. Struct Health Monit 2012;11:43–9. https://doi.org/10.1177/1475921710395815.

[12] Ing RK, Quieffin N, Catheline S, Fink M. In solid localization of finger impacts using acoustic time-reversal process. Appl Phys Lett 2005;87:1–3. https://doi.org/10.1063/1.2130720.

[13] Park B, Sohn H, Olson SE, DeSimio MP, Brown KS, Derriso MM. Impact localization in complex structures using laser-based time reversal. Struct Health Monit 2012;11:577–88. https://doi.org/10.1177/1475921712449508.

[14] Pahlavan L. Wave Propagation in Thin-walled Composite Structures: Application to Structural Health Monitoring. Technische Universiteit Delft, 2012.

[15] Yu Z, Xu C, Sun J, Du F. Impact localization and force reconstruction for composite plates based on virtual time reversal processing with time-domain spectral finite element method. Struct Health Monit 2023;22:4149–70. https://doi.org/10.1177/14759217231164297.

[16] Sanchez J, Benaroya H. Review of force reconstruction techniques. J Sound Vib 2014;333:2999–3018. https://doi.org/10.1016/j.jsv.2014.02.025.

[17] Inoue H, Harrigan JJ, Reid SR. Review of inverse analysis for indirect measurement of impact force. Appl Mech Rev 2001;54:503–24. https://doi.org/10.1115/1.1420194.

[18] Gaul L, Hurlebaus S. Determination of the impact force on a plate by piezoelectric film sensors. vol. 69. Springer-Verlag; 1999.

[19] Choi K, Chang FK. Identification of impact force and location using distributed sensors. AIAA Journal 1996;34:136–42. https://doi.org/10.2514/3.13033.

[20] Jacquelin E, Hamelin P. Force recovered from three recorded strains. n.d.

[21] Jacquelin E, Bennani A, Hamelin P. Force reconstruction: Analysis and regularization of a deconvolution problem. J Sound Vib 2003;265:81–107. https://doi.org/10.1016/S0022-460X(02)01441-4.

This work is licensed under CC BY 4.0

Media and Publishing Partner NDTnet

[22] De Simone ME, Ciampa F, Meo M. A hierarchical method for the impact force reconstruction in composite structures. Smart Mater Struct 2019;28. https://doi.org/10.1088/1361-665X/aae11c.
[23] Martin MT, Doyle JF. Impact Force Identification from Wave Propagation Responses. vol. 18. 1996.
[24] Berkhout AJ. Seismic Migration. 2nd ed. Elsevier; 1982.
[25] Pahlavan L, Blacquière G. Fatigue crack sizing in steel bridge decks using ultrasonic guided waves. NDT and E International 2016;77:49–62. https://doi.org/10.1016/j.ndteint.2015.09.006.
[26] De Luca A, Perfetto D, Lamanna G, Aversano A, Caputo F. Numerical investigation on guided waves dispersion and scattering phenomena in stiffened panels. Materials 2022;15. https://doi.org/10.3390/ma15010074.
[27] Saccone C, Pahlavan L. Influence of stiffeners and choice of transducers on the measurability of acoustic emissions in maritime structures. Struct Health Monit 2026. https://doi.org/10.1177/14759217251409328.
[28] Trethewey MW, Cafeo JA. Tutorial: Signal Processing Aspects of Structural Impact Testing. 1992.

This work is licensed under CC BY 4.0

Media and Publishing Partner